APPLICATION OF MULTI-AGENT COORDINATION METHODS TO THE DESIGN OF SPACE DEBRIS MITIGATION TOURS

Jeffrey Stuart[(1)], **Kathleen Howell**[(2)], **and Roby Wilson**[(3)]

[(1)]*Ph.D. Candidate, Purdue University, School of Aeronautics and Astronautics, 701 W. Stadium Ave., West Lafayette, IN, 47906, (765) 620-4342, jrstuart@purdue.edu*

[(2)]*Hsu Lo Distinguished Professor of Aeronautics and Astronautics, Purdue University, School of Aeronautics and Astronautics, 701 W. Stadium Ave., West Lafayette, IN, 47906, (765) 494-5786, howell@purdue.edu*

[(3)]*Supervisor, Inner Planet Missions Analysis Group, Mission Design and Navigation Section, Jet Propulsion Laboratory, California Institute of Technology, 4800 Oak Grove Dr., Pasadena, CA 91109, (818) 393-5301, roby.s.wilson@jpl.nasa.gov*

Abstract: *The growth in the number of defunct and fragmented objects near to the Earth poses a growing hazard to launch operations as well as existing on-orbit assets. Numerous studies have demonstrated the positive impact of active debris mitigation campaigns upon the growth of debris populations, but comparatively fewer investigations incorporate specific mission scenarios. Furthermore, while many active mitigation methods have been proposed, certain classes of debris objects are amenable to mitigation campaigns employing chaser spacecraft with existing chemical and low-thrust propulsive technologies. This investigation incorporates an ant colony optimization routing algorithm and multi-agent coordination via auctions into a debris mitigation tour scheme suitable for preliminary mission design and analysis as well as spacecraft flight operations.*

Keywords: *automated trajectory design, space debris mitigation, ant colony optimization, multi-agent auctions, vehicle routing problem*

1. Introduction

The current population of debris objects in Earth orbit, and the projected growth in the size of this population, are concerns to many governmental agencies, private companies, and other participants in the space industry. Debris objects pose a hazard to active spacecraft, often necessitating maneuvers to avoid dangerous close approaches, while collisions between debris objects have the potential to create a cascading build-up of debris in near-Earth orbit.[1] Indeed, in February 2009, an on-orbit collision occurred between an active Iridium communications satellite and a defunct Cosmos satellite wherein the Iridium satellite was lost and large amount of new debris objects were released.[2] At the same time, active anti-satellite system tests, such as the Fengyun-1C[3] and USA-193,[4] have contributed greatly to the debris environment. The Fengyun-1C test was particularly disruptive as it generated a large amount of debris in an already relatively highly-populated orbit.[5] Accordingly, satellite disposal policy and active debris removal campaigns are a focus of international discussion.

The long-term evolution of debris populations has been the focus of many analyses, and the improved accuracy in collision prediction and error estimation is a topic of on-going investigation. For example, Liou,[6] Loftus,[7] and Lewis[8] have demonstrated the positive effect of active debris mitigation on long-term debris populations. Likewise, many advancements have occurred in the detection, tracking, and characterization of artificial objects orbiting the Earth.[9,10,11,12] Less

attention, however, has focused on trajectory design and analysis to mitigate the existing debris objects, though Peterson[13] has published preliminary results that include the identification of high-priority debris objects and a ΔV cost analysis for disposal missions; furthermore, Castronuovo[14] and Braun et al.[15] have proposed preliminary debris mitigation mission concepts. These studies, however, typically presuppose a fixed order of target encounters or are restricted to general order-of-magnitude analyses. In contrast, scenarios wherein the targets and order are not pre-defined have, thus far, rarely been applied to the particular problem of debris mitigation, though recently Missel and Mortari have applied a genetic algorithm to path pre-planning[16] and Barbee et al. examined a model of the Traveling Salesman Problem.[17] Furthermore, Ceriotti and Vasile incorporated an ant colony optimization algorithm within a scheme to generate interplanetary gravity-assist trajectories.[18] On the other hand, market-based auction algorithms have been successfully applied to spacecraft constellation design and operations,[19,20,21] though they have yet to be applied to the mitigation of space debris or similar spacecraft routing problems.

An automated procedure to generate rendezvous tours for an active debris removal campaign is proposed wherein multiple spacecraft or "chasers" encounter and operate upon multiple debris objects. The mission design scenario for a single spacecraft can be modeled as a vehicle routing problem (VRP) where the goal is a spacecraft that encounters a large number of debris objects while being constrained in available propellant. However, since a single chaser can only encounter a limited number of debris objects, the use of multiple spacecraft operating as independent agents within a larger system is investigated. In particular, ant colony optimization[22,23] as well as auction and bidding processes[24,25] are examined as a method to coordinate the operation of the debris-mitigating satellites for both pre-mission planning and real-time adjustments to baseline designs. The chaser employs a chemical propulsion system while debris mitigation operations require some finite time interval in the close vicinity of the object, so transfer duration and spacecraft loiter time must also be addressed. Proximity operations at the debris objects are not explicitly modeled in this analysis but some assumed cost is applied at each encounter to represent these activities. Though this penalty potentially entails some additional propellant expenditure, the exact form of this cost depends heavily upon the objects under consideration. For example, a small object may be collected by a servicer spacecraft and, thus, increase the inert mass of the system. Alternatively, the main vehicle may deploy de-orbit packages at the larger objects, where this drop in mass can incur an additional penalty to the propellant expenditure. Furthermore, the servicer spacecraft is typically restricted to relatively short-term missions, as opposed to multi-year operations, such that large changes in the motion of the spacecraft must be generated via the on-board propulsion systems rather than natural but slow perturbations in the motion of the orbiting bodies. Though this analysis uses a simplified computational scheme that abstracts many of these considerations, preliminary target sequences and the expected mitigation costs may still be assessed. Furthermore, while this investigation does not explicitly consider launch or on-orbit resupply considerations, the proposed methods are readily modified to incorporate scenarios where the mitigation architecture includes a supply station or other "home-base" in addition to the chaser spacecraft.

2. Debris Classification and Mitigation Strategies

One critical element of debris mitigation is the identification and classification of potential target objects. While the technology to identify and track objects orbiting the Earth has existed for several

decades, only recently have attempts been made to produce a systematic classification scheme for artificial debris objects.[9,10,11] These taxonomic schemes draw upon many phsyical characteristics, from orbit regime to size and shape to material composition, to determine the origin, current status, and potential orbital evolution of the debris objects. A modified set of Früh's taxonomic categories for artificial satellites is detailed in Table 1; note that many of these classifications are available using remote observation techniques. Once the observed and inferred physical characteristics of an object have been collected, the long-term evolution and hazard level of the artificial satellite may be assessed. Red text in Table 1 indicates specific debris classifications that serve as a focues of this preliminary investigation. In particular, large objects that are more likely to contribute to the future growth of the debris population due to shedding and fragmentation events are preferentially targeted for removal. However, suitable modifications to the methodology and cost models could widen the design space to address additional debris types. Note that since proximity operations are not explicitly modeled, no restrictions apply to certain descriptor categories.

Table 1. Physical characteristics for taxonomic classification of artificial debris objects.

Descriptor	**Classification**			
Orbit regime	LEO	MEO	GEO	HEO
Orbit control	controlled / active		uncontrolled / defunct	
Attitude	controlled	spinning	tumbling	
Fragmentation	intact	fragment		
Material	single	few	composite of many	
Size	large (>1.5m)	medium	small (<10cm)	micro (<1cm)
Shape	regular convex	regular with concavities		irregular
Area to mass ratio (AMR)	high (HAMR) >2 m^2/kg	medium (MAMR)	low (LAMR) >0.8 m^2/kg	

As with the debris objects themselves, potential mitigation strategies may also be classified in terms of a variety of elements of the mission architecture. While an exhaustive survey of all currently proposed mitigation strategies has yet to be completed, an overview sufficient for the current investigation is included in Table 2. As in Table 1, red text indicates the assumed architecture for this investigation; note that the proposed tour generation strategies are readily modified to address a variety of mitigation strategies. Since not all mitigation strategies are technologically feasible for all debris types, multiple debris mitigation architectures are required to significantly reduce the debris population. Furthermore, even when a mitigation plan is crafted to target a specific portion of the debris population, economic realities may limit the full impact that such a strategy might realize. For example, an architecture based on chaser spacecraft rendezvous and subsequent deployment of de-orbit packages to multiple large debris objects within a short time frame, entails relatively high propellant costs and, therefore, necessitates either a large number of spacecraft or the presence of on-orbit supply depots for the chaser vehicles. Thus, while preliminary results indicate that the proposed mitigation strategy is capable of a significant reduction in the hazard posed by large debris objects within a relatively short time frame, the full impact is necessarily limited in scope and must be supplemented by alternate strategies targeting other debris categories.

Table 2. Potential components of debris mitigation architectures.

Descriptor	Classification				
Platform	spacecraft	launch vehicle	ground-based	balloon	aircraft
Time scale	<1 day	<1 year (short)	>1 year (long)		
TRL	9 - flight proven	7	5 - component validation	3	1 - basic principle
On-orbit propulsion	chemical	electric	solar sail	electrodynamic	none / NA
Disposal	atmospheric	graveyard orbit	reclamation		
Approach	rendezvous	fly-by	none / NA		
Interaction method	collision	dissipative	capture	deployable	
interaction method sub-descriptors	*destructive* *controlled*	*propellant exhaust* *gas cloud* *laser*	*tug* *scow* *slingshot* *net*	*tracker* *propulsive* *drag inducing* *solar sail* *electrodynamic tether*	

3. Selection of Target Debris Groups

Given the tens of thousands of debris objects in Earth orbit, careful selection of potential targets of interest is a necessary step in the formulation of a feasible mitigation strategy. Investigations by Peterson[13] and Lewis et al.[26] identify specific debris objects and categories that pose the highest long-term threat in terms of probability and severity of collision. These objects are typically large, intact objects such as defunct satellite buses or rocket bodies from the upper stages of launch systems. Furthermore, as demonstrated by Peterson, these high-risk objects usually form a taxonomic group in terms of physical characteristics such as orbit regime as well as body size and shape. In particular, the LEO regime is of great concern because of the high density of objects with large relative velocities and correspondingly high-energy collision events. On the other hand, LEO altitudes readily allow for the definitive termination of debris objects via atmospheric re-entry. Thus, a viable mitigation strategy for large LEO objects is the attachment of de-orbit packages such as propulsive modules or drag-inducing devices.

Based upon Peterson's analysis, a test case in this investigation is the active mitigation of the SL-8 / Kosmos upper stage rocket bodies. The identical size and shape of these target objects enables the easy replication of any needed chaser spacecraft attachment mechanism as well as the deployable de-orbit package. Indeed, the major distinquishing factor among the SL-8 rocket bodies is the orbital behavior of the objects. The vast majority of the 295 currently extant Kosmos upper stages (as of July 4^{th}, 2013) reside in nearly circular orbits with three distinct altitude / inclination groupings at roughly 760 km / 74°, 970 km / 83°, and 1570 km / 74°, as illustrated in Fig. 1. On the other hand, the target rocket bodies are widely distributed in right ascension of the ascending node (RAAN) and phase within their respective orbit planes.

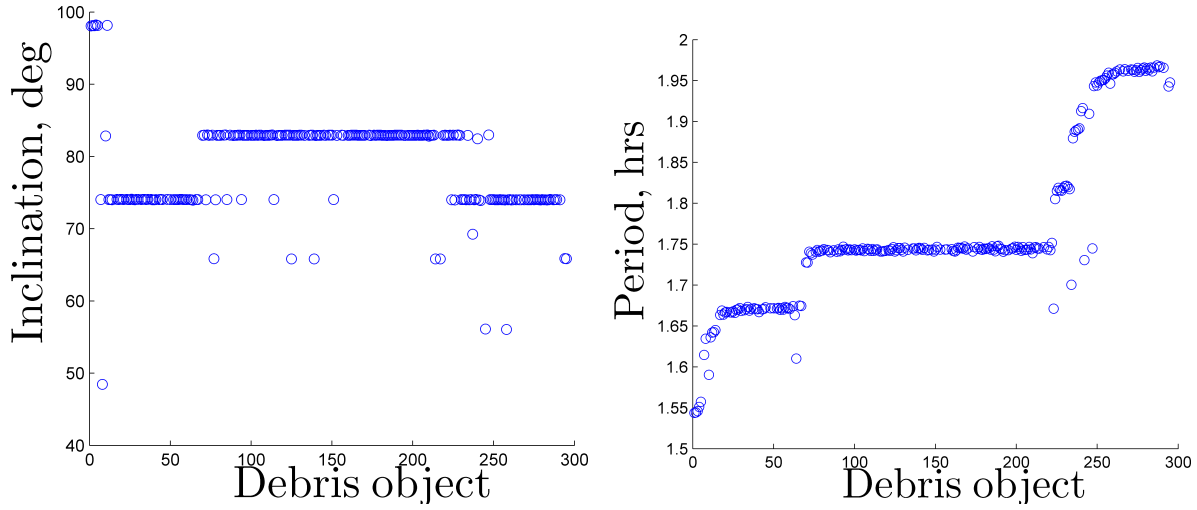

Figure 1. Orbital period and inclination with respect to the equator of the target SL-8 / Kosmos upper stage rocket bodies.

4. Computation of Estimated Rendezvous ΔV Cost

Due to the clustering of the target orbits in size, shape, and inclination, the majority of propellant expenditure for a chaser spacecraft traveling from one rocket body to another within the same group is due to the maneuvers to change the orbital plane as well as to match the phase of the destination object. That is, the total rendezvous cost can be approximated via

$$\Delta V = \Delta V_{pc} + \Delta V_{ph} \tag{1}$$

where ΔV_{pc} is the cost due to changes in the orbit plane and ΔV_{ph} is the cost of the phasing maneuvers. The plane change and phasing costs are assumed to be decoupled and only a simplified cost model is desired, hence, analytical expressions estimating the cost of chaser spacecraft rendezvous with the debris objects are readily developed for this preliminary analysis.

4.1. Plane Change ΔV Cost

For short-duration mitigation missions for which zonal drift and other pertubative effects are negligible, changes in the orbit plane must be accomplished via the expenditure of propellant. If the current and destination orbits intersect in physical space, then the transfer may be accomplished using a single impulse. Note that for the general case of intersecting orbits, the required magnitude of a single impulse ΔV_{si} maneuver is evaluated as

$$\Delta V_{si}^2 = V_D^2 + V_T^2 - 2V_D V_T \cos\eta \tag{2}$$

where V_D and V_T are the speeds along the departure and target orbits at the point of intersection, respectively. The angle η is the angle between the velocity vectors. Note that for the special case when departure and destination orbits are identical but for different planes of motion reflected in different nodal crossings (i.e., RAAN), the shift in the orbit plane is accomplished by a single impluse at one of the two intersection points of the orbital tracks. Furthermore, given the nearly

circular orbits in which the target rocket bodies reside, the cost to transfer between orbit planes is easily approximated as

$$\Delta V_{pc} = 2V_c \sin\frac{\Delta\Omega}{2} \tag{3}$$

where $\Delta\Omega$ is the difference in RAAN between the initial and arrival orbit planes and V_c is the circular orbit velocity, as illustrated in Fig. 2. Using this formulation, the cost of the transfer maneuver is estimated simply from the classical elements describing the target orbits without any requirement to locate the intersection points between the spacecraft paths. Recall the three groupings of debris bodies in Fig. 1. One object from each group is selected, where the plane change maneuver from the selected target to all other upper stages within its own group yields Fig. 3. Note that for all three families or groups, the cost associated with small values of $\Delta\Omega$ results in a nearly linear relationship between $\Delta\Omega$ and ΔV, as expected, and requires approximately 1 km/s enabling about 8° change in RAAN.

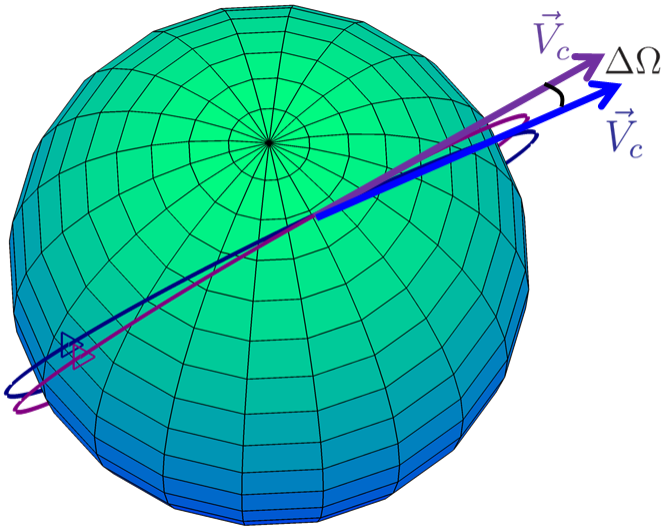

Figure 2. Intersection velocities of departure (blue) and target (purple) debris orbits. Note that difference in RAAN $\Delta\Omega$ is equal to the angular difference between the two velocities.

4.2. Phasing ΔV Cost

While shifting the orbital plane of the chaser spacecraft to that of the target rocket body is a necessary step in the rendezvous process, the required maneuver that is necessary to match the phase of the debris object must also be incorporated into the cost model. Due to the low eccentricity of the derelict upper stages, differences in phase are straightforwardly expressed in terms of changes in the argument of latitude, $\Delta\theta$, that is, the varying times associated with the object's crossing of the equitorial plane of Earth. One strategy to match the phase of the chaser to that of the target is a boost of the chaser spacecraft into a loiter orbit with a different period from that of the debris object and wait until the differences in mean motion bring the chaser and target within close proximity. After any difference in argument of latitude is eliminated, a second burn returns the chaser spacecraft to a circular orbit matching the orbit of the debris object. A notional respresentation of this process appears in Fig. 4, where the number of revolutions, n, of the chaser spacecraft on the phasing ellipse

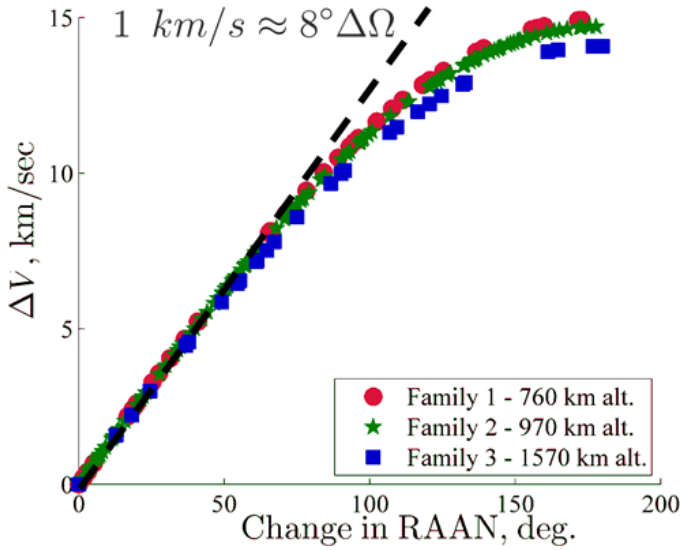

Figure 3. Plane change costs for three SL-8 rocket body groupings. For low changes in RAAN the cost is approximately linear.

and, m, the target object on its circular path are independently adjustable. The required period of the phasing orbit occupied by the chaser, $\mathbb{P}_E$, is computed via

$$n\mathbb{P}_E = \mathbb{P}_C\left(m + \frac{\Delta\theta}{2\pi}\right) \tag{4}$$

where $\mathbb{P}_C$ is the period of the debris object in the circular orbit and the difference in the argument of latitude, $\Delta\theta$, between the chaser and target varies between $\pm\pi$ radians. The integers n and m represent the number of revolutions n of the chaser spacecraft along the phasing orbit and the revolutions m of the debris object in the target orbit. Once an appropriate size for the phasing orbit is determined, the total propulsive cost for the phasing maneuvers is

$$\Delta V_{ph} = 2\|V_E - V_C\| \tag{5}$$

where V_E is the speed on the phasing ellipse at the circular orbit altitude, i.e., at either periapse or apoapse depending upon whether the debris object is trailing or leading the chaser spacecraft, respectively. Recall that two burns are required for phasing, hence the factor of 2 in Eq. (5). The relevant apse speed on the phasing orbit is obtained from

$$V_E = \sqrt{\frac{2\mu}{a_C} - \frac{\mu}{a_E}} \tag{6}$$

where the elliptical and circular semi-major axes a_E and a_C are calculated via

$$\left(\frac{\mathbb{P}}{2\pi}\right)^2 = \frac{a^3}{\mu}, \tag{7}$$

with $\mu = 3.986 \times 10^5 \frac{km}{s}$, the gravitational parameter for the Earth.

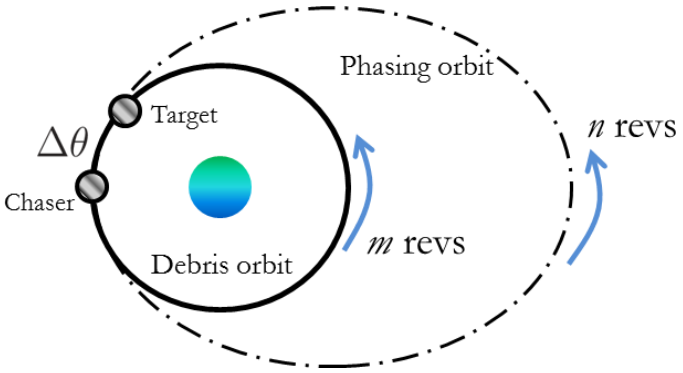

Figure 4. Illustration of debris object orbit and phasing orbit for the spacecraft. If the debris object leads the chaser spacecraft, a phasing orbit smaller than the debris orbit is used.

A trade-off between the phasing and debris orbital periods and propellant cost is available for the phasing portion of the rendezvous maneuvers. The revolution numbers n and m in Eq. (4) can be independently adjusted, but, if more than one phasing revolution about the Earth is incorporated, the most successful strategy maintains $n = m$ so that differences in orbital periods and, consequently, the required propellant expenditures, are reduced. Thus, the trade-space for a single shift in orbit phasing from one debris object to another is reduced to simply the balancing of the duration, represented by the number of phasing revolutions n, and the required ΔV from the propulsion system. The phasing maneuver costs across the three target groupings and for two phasing durations, $n = 10$ and $n = 100$, are plotted in Fig. 5. Note the linear relationship between ΔV and number of phasing revolutions as well as cost and the required change in argument of latitude. These linear relationships break down if the phasing maneuver is attempted for a low number of orbital periods. For this preliminary investigation, the revolution number n is fixed for any particular solution run, however more sophisticated search methods incorporating both transfer time and cost could be implemented.[27]

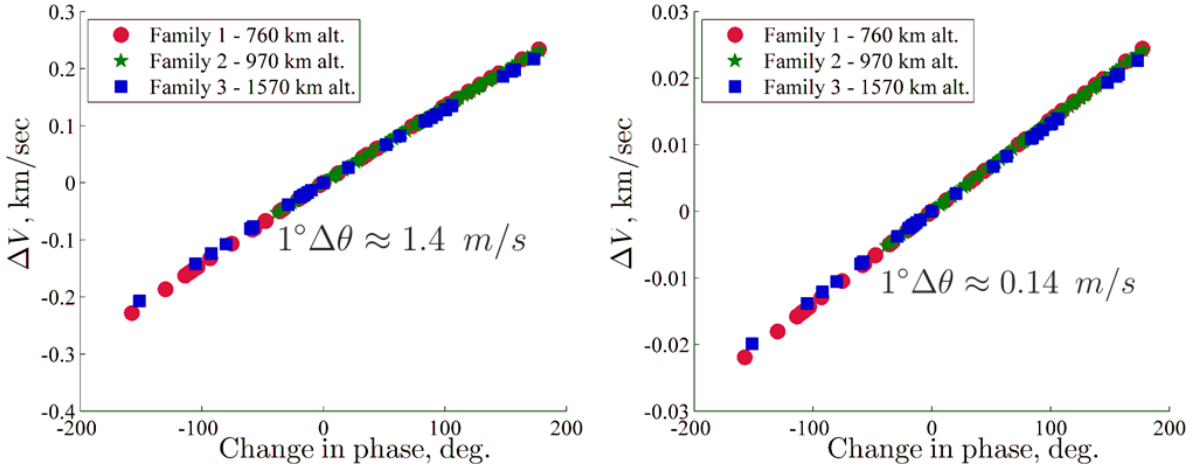

a. ΔV cost for 10 periods, $n = m = 10$. b. ΔV cost for 100 periods, $n = m = 1$.

Figure 5. Phase change cost for three SL-8 upper stage families.

5. Routing and Coordination Algorithms

Due to limits on propulsive capability and the number of de-orbit packages on the chaser spacecraft, multiple mitigation spacecraft are required to encounter and remove a significant number of target objects in a short time frame. The need for multiple chasers combined with the large number of potential targets presents a large solution space for which efficient, automated tour generation strategies are a key enabling factor in the design of mitigation missions. In this investigation, the meta-hueristic search algorithm denoted ant colony optimization (ACO)[22,28] is applied as a path planning tool for preliminary misison design. This search algorithm is well-suited for vehicle routing problems (VRP), e.g., spacecraft tour generation, and enables the selection of efficient mitigation tours prior to on-orbit spacecraft insertion. However, when the chaser spacecraft perform in a flight operational mode, the evolving dynamical environment of the LEO debris population may necessitate the rapid formulation of a new target sequence. While this operation can be accomplished using ACO, another resource allocation algorithm, an auction and bidding method,[24,25] is proposed for the real-time alteration of tour mitigation sequences.

5.1. Ant Colony Optimization

Ant colony optimization (ACO) is a stochastic route-finding algorithm patterned after the foraging behavior of ant colonies wherein ants alternately explore for food and follow pheromone trails to known food sources. Once a food source is discovered, the ants instinctively locate a route that is near-optimal in travel distance to the food while retaining the ability to adapt to changing environments and opportunities. The process relies on the continued creation and dissipation of pheromone trails such that favorable trails are reinforced while other routes decay due to lack of use. This process is inherently robust while ensuring close-to-optimal performance as well as an allowance for a variety of static and dynamic applications. One natural application for ACO is the solution of vehicle routing problems (VRP);[29,23] the generation of debris mitigation tours is a specific example. However, one critical factor incorporated into any search strategy is the fact that the chaser spacecraft is not infinitely capable but instead possess limited propulsive reserves and mitigation capability, here represented by the on-board number of de-orbit packages.

Simple vechicle-routing ACO applications assume a discrete set of N targets, or nodes, with single, bi-directional links, such that an "ant" traveling from location A to location B can easily travel equally in the opposite direction for the same cost. As illustrated in Fig. 6, these networks are usually sparse, that is, not every pair of nodes is connected. In most applications, the goal is to traverse the network from one node to another or to create a circuit of all nodes, in both cases, for the least cost. However, for debris mitigation spacecraft with limited capability, the network-spanning route is split into discrete sequences that can be addressed by one individual vehicle. In this case, an "ant" representing a chaser spacecraft traverses all potential debris targets with a "reset" after a chaser spacecraft has exhausted either its propellant (ΔV_{cap}) or de-orbit package (p_{cap}) reserves. For an individual ant, the number of resets is equivalent to the number of chaser spacecraft required to implement all encounter sequences that the ant follows. This concept is notionally presented in Fig. 6, where the dashed, colored links indicate sequences followed by individual chaser spacecraft (the "ant", in turn, travels all dashed connections). For this investigation, the target-to-target transfer model is simplified to one ΔV cost as given by Eq. (1). Recall that the plane-change cost is

determined entirely by the geometry of the target debris orbits while the phasing cost is dependent upon the selection of the phasing number n.

The ant colony algorithm mimics the foraging behavior of ant colonies by performing a series of parallel searches wherein sets of virtual ants construct individual routes through the network. During each round of parallel searches, termed a "generation", multiple ants are released such that the individual ants construct independent sets of encounter sequences. Thus, to construct routes during the k^{th} generation, each individual ant, after placement at a random initial object, travels from node to node by following these behavioral rules at each encountered node:

1. *Exploration*: With some probability γ, the "ant" travels to a randomly selected new node, where the parameter γ decreases from 1 to some steady-state value $0 < \gamma_{ss} < 1$ over succeeding generations; else,
2. *Following*: Stochasitcally select an unvisited node with the probability

$$P_{i,j} = \frac{\tau_{i,j} B_{i,j}^{\beta}}{\sum \tau_{i,j} B_{i,j}^{\beta}} \tag{8}$$

   where $P_{i,j}$ is the probability for travel from the i^{th} node to the j^{th} node, $\tau_{i,j}$ is the pheromone level on the link, $B_{i,j}$ is the quality of the connection, and β is a weighting parameter.
3. *Reset*: If the chaser spacecraft exhausts either its set of de-orbit packages or propellant capacity, place the ant at a randomly selected unvisited debris object with full mitigation and propellant capacities.
4. When all nodes / debris objects have been traversed, terminate search for the individual ant. The total number of resets that the ant must perform represents the number of chaser spacecraft required to affect the constructed mitigation sequences.

Once each individual ant has completed its search for the k^{th} generation, global information on successful routes is conveyed to succeeding generations via the creation and dissapation of virtual pheromones. The number of ants released in each generation, i.e., N_a, is an adjustable parameter in the algorithm. For the current implementation of ACO, the exploration probability in the k^{th} generation is defined to be

$$\gamma = \gamma_{ss} + (1 - \gamma_{ss}) e^{-\frac{k-1}{\ln N_g}} \tag{9}$$

where γ_{ss} is the lowest desired exploration probability and N_g is the total number of generations over which the search will be performed. This definition of exploration probability ensures a smooth exponential decay from a probability of 1 in the first generation to the base probability, γ_{ss}. The term involving the natural logarithm provides a consistent decay of exploration likelihood regardless of the number of generations. In this investigation, the individual link quality is defined

$$B_{i,j} = \Delta V_{a:i \to j} = \Delta V_{cap} - \sum \Delta V_p \tag{10}$$

where $\Delta V_{a:i \to j}$ is the remaining propulsive capability of the chaser spacecraft at arrival at the target object, ΔV_{cap} is the initial mitigation spacecraft propellant reserve, and $\sum_{\Delta V_p}$ is the summed propellant expenditure for the links previously followed by the spacecraft. Note that while the current investigation simplifies the link quality to an evaluation of the ΔV cost, previous studies

have successfully incorporated travel time and the importance of the target objects into the link quality metric.[27]

Global information on beneficial routes through the network are conveyed to individual ants via the creation and dissapation of pheromone values associated with specific object-to-object transfer options. This updated pheromone represents a transfer of information from one generation of ants to the next such that ants in later generations possess a higher probability of generating higher-value encounter sequences. After each succeeding generation of ants, the pheromone levels along each individual link are updated via

$$\tau_{i,j} = (1-\rho)\tau_{i,j} + Q_{i,j} \tag{11}$$

with a decay rate ρ and a pheromone update $Q_{i,j}$. Furthermore, if the pheromone level on an individual link falls below a certain threshold, ρ_L, the pheromone level on that transfer option is set to zero. This procedure removes the need to explicitly compute travel probabilities that are already nearly zero as compared to trails with higher reinforcement levels. Note that the pheromone increase, $Q_{i,j}$, corresponding to a given link is either zero (if only the best routes and, therefore, the best links, are reinforced) or some function that is dependent on the performance metric associated with tours that include the particular leg in question. In this investigation, the pheromone update procedure increases the pheromone on each link of the current best tour over all previous generations by the value $1/Q$ where the quality value Q is defined to be

$$Q = C_{sc}N_{sc} + \sum_{k=1}^{N_{sc}} \Delta V_k \tag{12}$$

where N_{sc} is the number of spacecraft or, equivalently, the number of "resets" required to encounter all debris objects, C_{sc} is a constant scaling factor, and ΔV_k is the propellant consumed by the k^{th} chaser spacecraft. The scaling constant C_{sc} is essentially a weighting factor that, if set sufficiently high, allows the number of required chaser spacecraft to dominate the propellant consumption, that is the total ΔV expenditure, of the individual spacecraft. Under this update model, the best tour acquires the lowest Q value. After a pre-determined number of generations, this procedure is terminated and the best tour is returned. Due to the stochastic nature of the algorithm, and the recognized tendency of ACO algorithms to quickly "lock" onto potential solutions, several runs are typically completed and the best route from among the runs is returned as the solution. For ACO algorithms as a whole, local information is supplied by the link quality, $B_{i,j}$, while global "goodness" information is preserved in the pheromone concentrations, $\tau_{i,j}$.

5.2. Auction and Bidding Methods

A bidding and auction process is applied to the coordination and modification of the debris removal sequences for multiple service spacecraft. In these auctions, individual spacecraft bid to remove specific debris objects through simple serial auctions where all available spacecraft bid to select the next object to visit. Under nominal conditions, the top bid collected from each spacecraft is then the next target object along their baseline routes as determined by the ACO scheme. However, for certain contingencies, e.g., a particular debris object is determined to pose an imminent threat of collision or a chaser spacecraft becomes deactivated, the auction process alters the operation of the

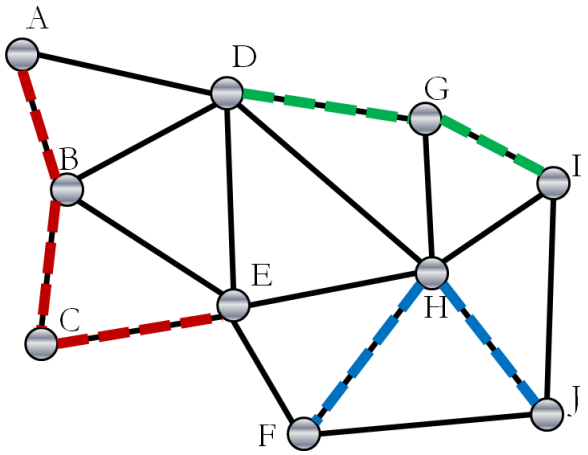

Figure 6. Schema of a sample debris network on which ant colony optimization can be applied. Links between objects can be traveled in both directions. Colored, dashed connections are traversed by specific chaser vehicles.

spacecraft swarm in real time. Note that, for the auctions in this investigation, no advantage ensues by under-bidding but over-bidding may offer benefits (e.g., a servicer can increase the attractiveness of its bid by underestimating the propellant cost). Therefore, this process is not currently "incentive compatible", i.e., honesty may not be the best bidding strategy for an individual spacecraft.[24] However, in this investigation, the mitigation spacecraft are assumed to be honest, a reasonable assumption when all chasers are operated by the same company or agency. In the event that the spacecraft are operated by competing entities, a system of salvage rights could be instituted in which the "owner" of the debris object sells the rights to recover valuable resources to the highest bidder, a system that would be incentive compatible.

A key element of the auction process is the bidding function; an appropriate choice incorporates one or more performance metrics from the current problem. For tours encountering and mitigating debris objects, several important considerations include: the propulsive capability of the chaser spacecraft, the ability of the spacecraft to physically handle the object, the relative threat posed by the debris objects, and the time-to-rendezvous and deploy a de-orbit package on the target object in question. Recall that the phasing duration is pre-selected and, therefore, translated into an equivalent ΔV cost. Accordingly, a bidding function is defined for the case when the k^{th} spacecraft bids upon the j^{th} object, namely

$$B_{j,k} = w_j^W \, p_k^R \Delta V_{k:i\to j}^M \tag{13}$$

where the bid B is a function of the relative threat posed by the object (w), the number of de-orbit packages remaining on the servicer spacecraft (p) after mitigating the target object, and the remaining propulsive capability (ΔV_k) after the servicer transfers from its current (debris object) orbit to the target orbit, as computed by Eq. 10. The weighting parameters W, R, and M are adjusted to modify the relative importance of each metric on the overall bid. Note, also, that if one of the weighting parameters is equal to zero, the bidding function is then insensitive to that particular metric. If equal weighting is used in this bidding function, the auction process favors the removal of the highest threat objects using the most capable spacecraft, i.e., the vehicle assuring the highest likelihood of success.

A serial, simple auction is implemented, wherein bids are solicited at periodic intervals Υ. The simple auction process is advantageous in that it is decentralized as well as relatively flexible and robust in the event of a chaser spacecraft failure or the addition of debris objects. Furthermore, updates to the object threat w are readily computed and incorporated into the bidding process. The process for the simple auction during each bidding period is as follows:

1. All hazard levels posed by the target objects are reassessed and communicated to the chaser spacecraft, also termed "agents".
2. If a chaser spacecraft is busy, either traveling between debris objects or currently mitigating a target object, it does not bid.
3. If a chaser is not busy, then it constructs bids on all debris objects within a reachable domain.
4. The agent then reports its top n bids, where n is the number of other chaser spacecraft participating in the auction process.
5. Each spacecraft that bids is first assigned its top bid. In the case that another spacecraft places a higher winning bid on the same object, then the losing agent is assigned to its second highest bid, etc.
6. In the event that several bids are equal, the assignment of targets is random.

Once an agent has been awarded a specific target, the spacecraft transfers to the orbit of the debris object, expending the required propellant ΔV. Furthermore, a de-orbit package is deployed to mitigate the debris object. Note that, in the bidding process, debris objects that have been assigned to a specific servicer spacecraft are then removed from future bids, even if the rendezvous and mitigation of the rocket body has not been completed. Larger values of Υ increase the likelihood of simultaneous bids. For this investigation, the value of Υ is set to a value such that all chaser spacecraft complete the mitigation of their respective targets before a new round of bidding is announced. Though not specifically modeled, one intriguing application is a modification of the auction such that an auction is called only when a high collision risk conjunction event is detected. The spacecraft follow their nominal routes constructed from the ACO process and only adjust behavior at the appearance of an imminent threat. The simple auction process is advantageous in that it is decentralized and relatively flexible and robust in the event of a chaser spacecraft failure or the emergence of additional debris objects. Furthermore, updates to the object threat value w is readily computed and incorporated into the bidding process.

6. Results

Potential tour sequences are generated and analyzed in terms of the required number of mitigation spacecraft as well as the performance of individual chasers. Ant colony optimization is employed to create preliminary encounter paths and determine the required number of spacecraft for complete mitigation of the target families. Auctions, on the other hand, are implemented to coordinate the actions of a more feasible number of chaser spacecraft under changing mitigation priorities. Initial target objects for the auction sequences are extracted from the results of the ACO analysis such that the debris objects offering the best possiblity for extensive mitigation sequences are preferentially targeted.

6.1. Preliminary Tour Sequences via ACO

The ACO algorithm is employed to generate potential tour sequences for each of the three sets of target debris objects. Recall that the ACO algorithm, in addition to creating routes for individual chaser spacecraft, assesses the total number of spacecraft that are necessary to mitigate all the debris objects in a given family. For this investigation, the same search parameters (e.g., spacecraft propellant capacity, number of ants, decay rate) are applied to each debris grouping. These parameters are detailed in Table 3.

Table 3. Spacecraft, tour, and ACO parameter values, common to all runs.

Quantity	Value
Propellant capacity of chaser spacecraft (ΔV_{cap}), km/s	2
Number of de-orbit packages per chaser spacecraft (p_{cap})	8
Phasing revolution number, $n = m$	30
Number of generations (N_g)	100
Number of ants (N_a)	20
Link quality weight in link probability (β)	1
Pheromone decay rate (ρ)	0.05
Pheromone lower threshold (ρ_L)	10^{-5}
Base exploration probability (γ_{ss})	0.1
Spacecraft number scaling factor, (C_{sc})	10

6.1.1. Family 1 - 760 km altitude

Tours are generated for the mitigation of the 39 SL-8 rocket bodies residing in 760 km altitude orbits. Recall that each tour, or "ant", respresents mitigation sequences for multiple chaser spacecraft. The performance of individual ants is examined in Fig. 7, where the required number of spacecraft for full removal of the target grouping as well as the average propellant per chaser are plotted for the last generation of the ACO run. The "Tour Number" is, in fact, the "ant" number. Across all the tours (ants), note the variance in the number of spacecraft required to accomplish the goal. Furthermore, there is an inverse relationship between the average ΔV expended per ant and the required number of chasers. This result supports the intuitive notion that chaser spacecraft with higher propulsive capability could generally reduce the required number of spacecraft for full mitigation. Similar trends are observed for the other target groupings at 970 and 1570 km altitudes.

Examination of the best mitigation tour, as produced by the ACO algorithm in the 45^{th} generation, reveals that a minimum of 13 spacecraft are necessary for complete, short-term mitigation of all members of the 760 km altitude family. While this number is economically infeasible, a smaller set of mitigation spacecraft could still result in a significant reduction in the population of upper stages. Figures 8 and 9 aid in identifying particular high-return-on-investment sequences; information on the individual performance of specific spacecraft is conveyed in Fig. 8 whereas Fig. 9 illustrates the clustering in the orbit planes for the encounter sequences. Two particular spacecraft, numbers 5 and 6 in the figures, encounter 4 and 5 debris objects in two distinct RAAN regions, 17° and 262°, respectively. Note that neither chaser reaches the propellant cap of 2 km/s or the de-orbit package capacity of 8. Yet, these two sequences present the best options for short-term, chemical-enabled

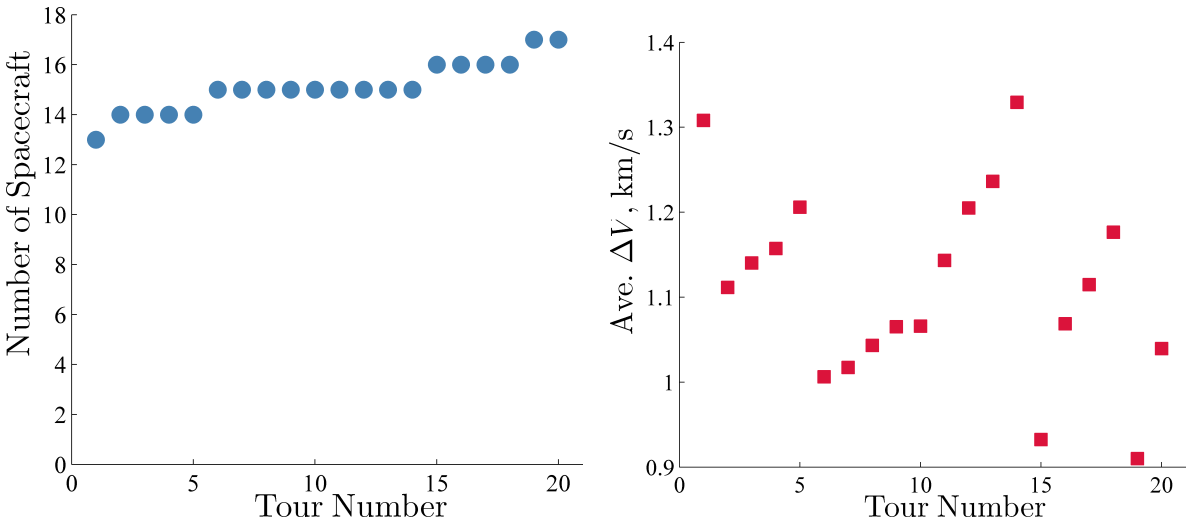

(a) (b)

Figure 7. "Ant" performance at last generation of ACO tour generation for 760 km altitude SL-8 rocket bodies.

mitigation of the selected objects; other mission architectures could increase the performance of the chaser spacecraft by incorporating more efficient propulsion systems, by exploiting long-term drifts due to spherical harmonics, or incorporating resupply depots for the chaser spacecraft.

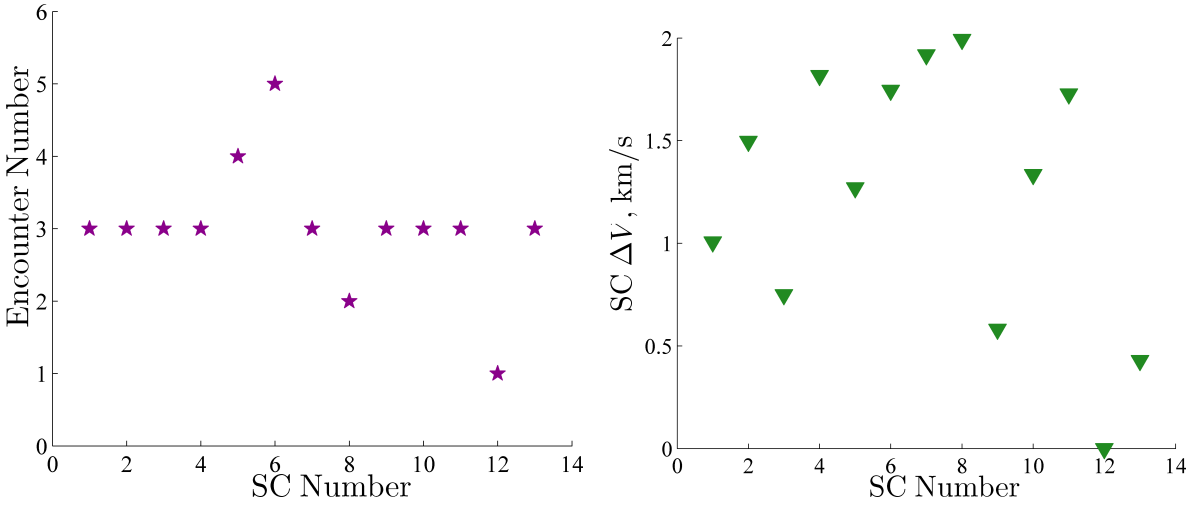

(a) (b)

Figure 8. Number of encountered debris objects and ΔV expenditure for each chaser spacecraft along the best found tour of 760 km family.

6.1.2. Family 2 - 970 km altitude

The ACO heuristic selection strategy is applied to the mitigation of the 114 upper stages in the 970 km altitude regime, where the best constructed tour, from the 98^{th} generation, requires 26 chaser spacecraft for full removal of the targets. As before, this number of spacecraft is currently not realizable, however Figs. 10 and 11 reveal several possibilities for high-return mitigation progressions. Two sequences exhaust all de-orbit packages on their respective carrier spacecraft,

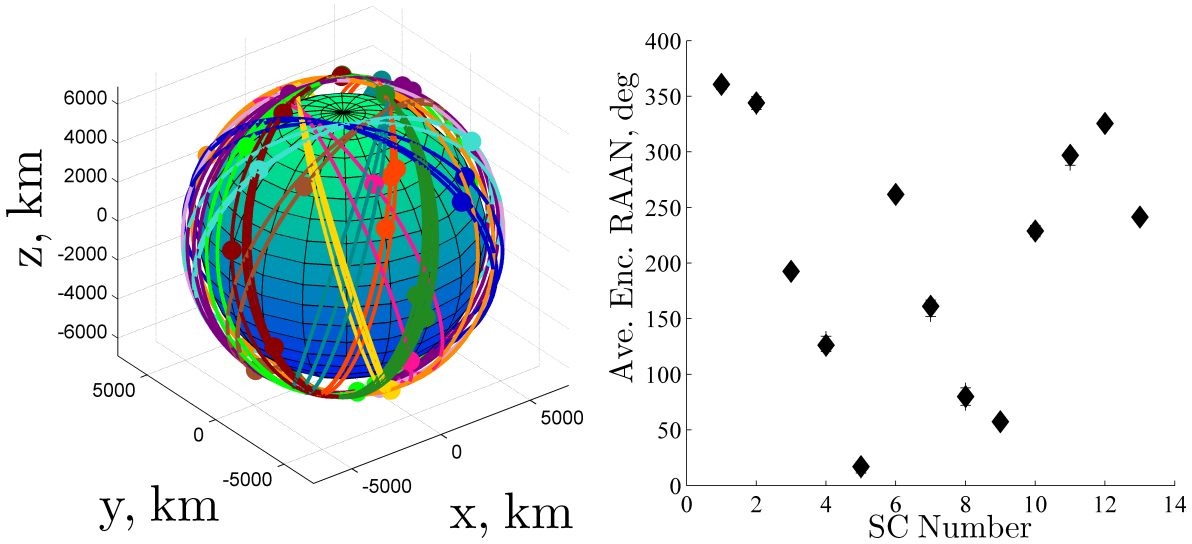

(a) (b)

Figure 9. Orbits and mean RAAN of encountered debris objects for each chaser spacecraft along the best found tour of 760 km family. Color of orbit indicates mitigation by different chaser spacecraft. Diamonds are average RAAN across all encounters while crosses indicate specific RAAN values.

while nearly half of the followed routes actually encounter 5 or more debris objects. Furthermore, most of the tour sequences expend more that three-quarters of the chaser propellant reserves, indicating that a moderate increase in propulsive capability could significantly reduce the number of spacecraft required. Likewise, mitigation of this target grouping, in particular, may benefit heavily from the use of refueling stations or other home-base architectures.

6.1.3. Family 3 - 1570 km altitude

The 29 target objects at the 1570 km altitude are examined for potential mitigation tours. The best tour emerged from the ACO procedure in the 52^{nd} generation and requires 13 chaser spacecraft for complete mitigation. Similar to the previous examples, Figs. 12 and 13 reveal the best potential for high-return encounter sequences. As in the mitigation tours for the first target family, two spacecraft encounter 5 and 4 debris objects, respectively, in two distinct RAAN regions, centered on 341° and 47°. Other than these two moderate encounter counts, all other potential spacecraft progressions in this region encounter a maximum of 2 upper stages, indicating a critical need to incorporate either long-term relative RAAN drift or a similar enabling architecture for the full depletion of this debris reservoir.

6.2. Adjusted Sequences via Auctions

While the ACO search algorithm reliably produces high-value target sequences, the auction coordination method readily re-routes chaser spacecraft to address contingencies such as the detection of an imminent conjunction with a high probability of physical collision. As a sample case, the auction process is applied to the mitigation of rocket bodies in the median altitude grouping at 970 km. Whereas the current best set of sequences from the ACO algorithm require a fleet of 26

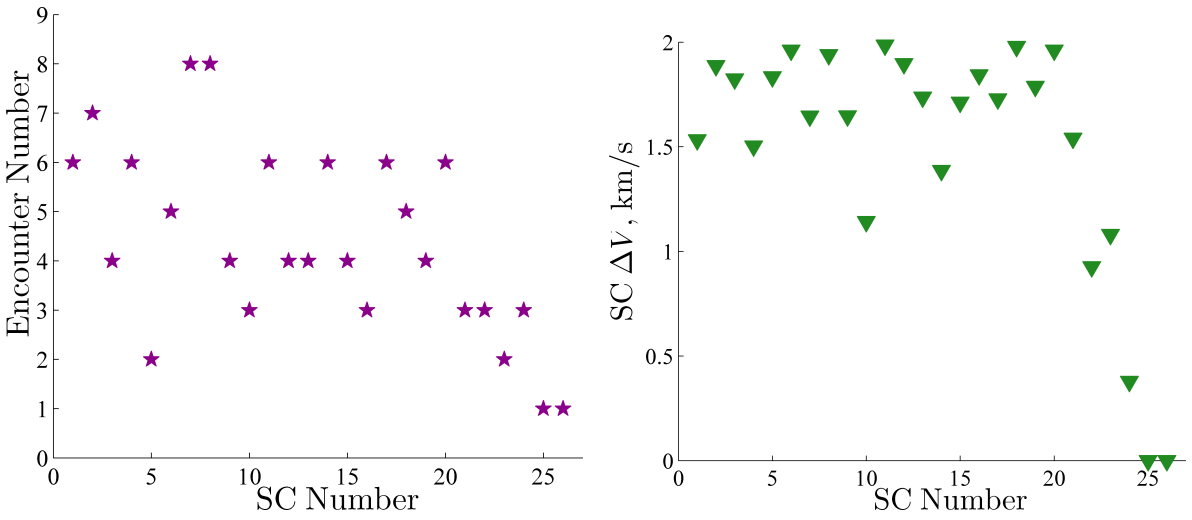

(a) (b)

Figure 10. Number of encountered debris objects and ΔV expenditure for each chaser spacecraft along the best found tour of 970 km family.

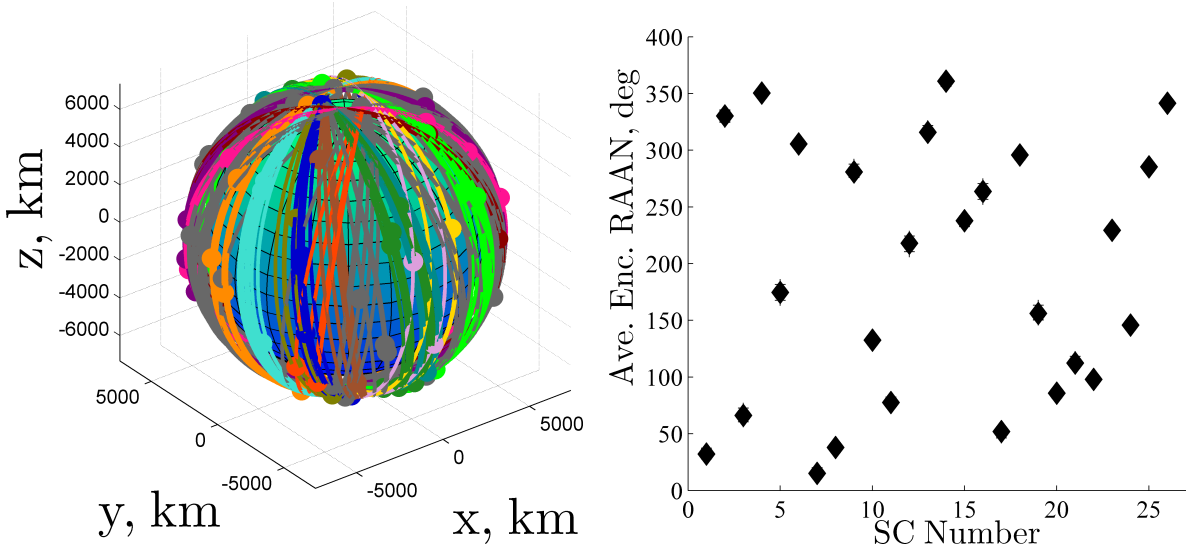

(a) (b)

Figure 11. Orbits and mean RAAN of encountered debris objects for each chaser spacecraft along the best found tour of 970 km family. Color of orbit indicates mitigation by different chaser spacecraft, up to the 15^{th} chaser. All subsequent encounters are plotted in grey. Diamonds are average RAAN across all encounters while crosses indicate specific RAAN values.

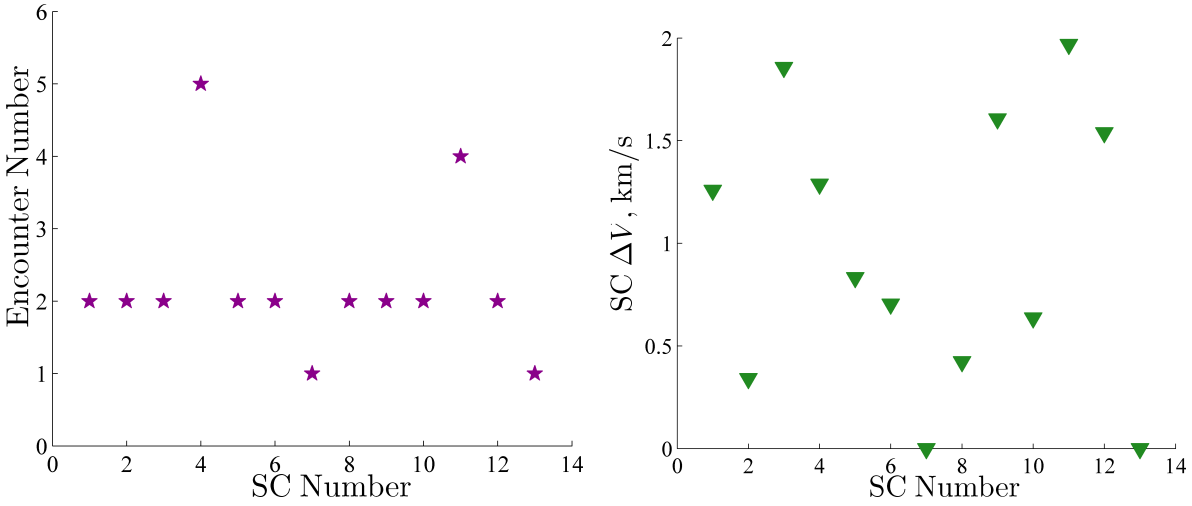

(a) (b)

Figure 12. Number of encountered debris objects and ΔV expenditure for each chaser spacecraft along the best found tour of 1570 km family.

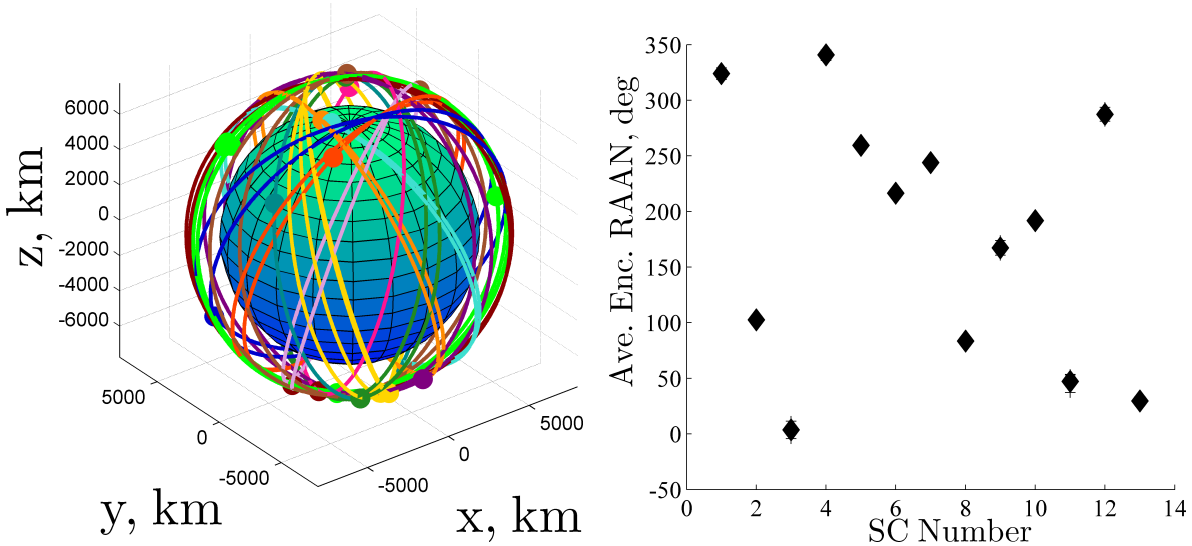

(a) (b)

Figure 13. Orbits and mean RAAN of encountered debris objects for each chaser spacecraft along the best found tour of 1570 km family. Color of orbit indicates mitigation by different chaser spacecraft. Diamonds are average RAAN across all encounters while crosses indicate specific RAAN values.

chaser spacecraft for complete mitigation of this target family, a more feasible set of 6 mitigation spacecraft is used in the auction algorithm. While this number of chasers is still somewhat large, the resulting interactions between the six spacecraft highlight several of the advantages of the auction and bidding process. For the auction runs, the initial targets of the highest performing chaser spacecraft from the previously conducted ACO search are also specified as the initial target objects of the bidding spacecraft; information on the 6 selected baseline sequences is summarized in Table 4. The subsequent path of the chaser spacecraft is determined solely by the auction and bidding process. At the initiation of each round of bidding, the threat level w_j posed by each debris object is randomly assigned from a uniform distribution on the interval [0.5, 1.5]. This changing target importance, selected as an extreme example, is formulated on purpose to illustrate the capability of the auction algorithm to address a highly dynamic problem space.

Table 4. Baseline target sequences from ACO tour generation within target family at 970 km altitude.

Auction SC Num.	**ACO SC Num.**	**Num. Enc.**	**Ave. RAAN, deg.**	**ΔV, km/s**
1	7	8	16	1.646
2	8	8	38	1.940
3	2	7	330	1.887
4	1	6	32	1.533
5	4	6	350	1.503
6	11	6	78	1.985

Two auction cases are tested: (i) one incorporating only the propellant and de-orbit package margins of the chaser spacecraft as well as (ii) one case that additionally includes the current debris hazard level. In both cases, the appropriate weighting factors M, R, and W in Eq. (13) are set to either 1 or 0 depending on the case. The results of the auction algorithm are summarized in Table 5, along with a comparison of the equivalent results from the ACO sequence generation process. As is apparent, the auctioned sequences without incorporation of the threat level, outperform the ACO progressions in terms of propellant consumption and the number of rocket body encounters. This improved outcome highlights two key considerations when using this particular implementation of ACO: i) while good target sets might be identified, the possibility always exists that individual spacecraft performance might be improved by adjusting its encounter sequence; and ii) even though the total required number of spacecraft are reliably predicted, individual targets may potentially be shifted from one chaser queue to another. In contrast, when the hazard level is incorporated into the bidding, the chaser spacecraft encounter fewer rocket bodies, but at a higher ΔV cost. However, those objects that are encountered are, on average, those with the highest removal priority. The performance of the individual chaser spacecraft is illustrated in Figs. 14 and 15. Two chaser spacecraft, in particular, auction spacecraft numbers 2 and 4, are the source of all the conflicting bids that must be resolved via the auction algorithm. These two chaser spacecraft operate largely within the same RAAN region - at nominal RAAN values of 38° and 32°, respectively - and often target the same debris objects, particularly when threat level is incorporated into the bid. The respective targets orbits are colored orange and blue in Figs. 14 and 15.

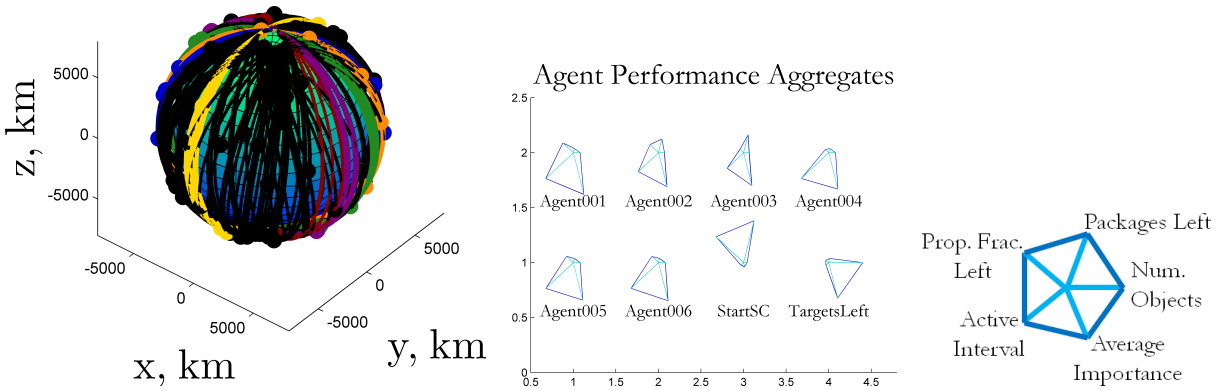

(a) Orbits (b) Relative Performance (c) Key

Figure 14. Mitigation sequences and agent performance resulting from auction process for 970 km altitude targets, threat omitted from bid (M=R=1,W=0). Glyphs indicate performance relative to other chaser spacecraft ("agents") as well as a spacecraft before any mitigation actions and the remaining debris population.

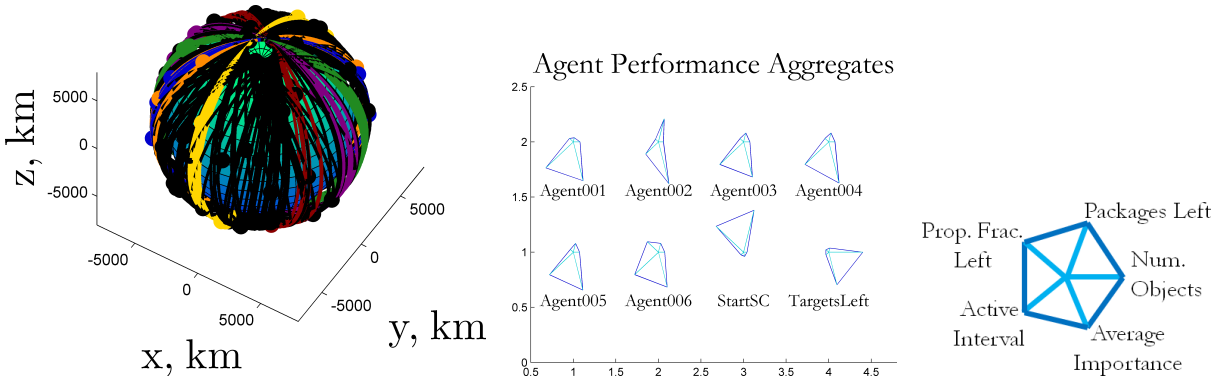

(a) Orbits (b) Relative Performance (c) Key

Figure 15. Mitigation sequences and agent performance resulting from auction process for 970 km altitude targets, threat including in bid (M=R=W=1). Glyphs indicate performance relative to other chaser spacecraft ("agents") as well as a spacecraft before any mitigation actions and the remaining debris population

Table 5. Performance comparison of ACO and auction methods, 6 chaser spacecraft, target family at 970 km altitude.

Quantity	Solution method		
	ACO	Auction M=R=1,W=0	Auction M=R=W=1
Total number of objects mitigated*	41	43	40
Average consumed ΔV, km/s	1.749	1.694	1.842
Average threat mitigated†	–	1.04	1.18
Number of conflicting bids	–	1	3

*From total of 114 orbiting debris objects.

†From uniform distribution over range [0.5,1.5].

7. Conclusions

A classification scheme for space debris mitigation architectures is proposed. While no one mitigation method is suitable for all types of debris objects, strategic selection of target objects and enabling technologies can yield a significant positive impact on the current size and future growth of the debris population. A preliminary test case generates feasible mitigation tours for short-term, chemically-propelled chasers targeting the expended upper stages of the SL-8 / Kosmos launch system. Two novel search and coordination strategies, ant colony optimization and auctions, have been implemented and tested using a simplified cost model. The proposed mission design strategy employs ant colony optimization for the preliminary generation of tours of interest as well as determination of the total number of chaser spacecraft required for complete mitigation of the target populations. Building upon this preliminary search, the auction and bidding process adjusts the previously constructed rendezvous sequences in a real-time, flight operation scenario. Notably, auction implementations both enhance the performance of specific baseline progressions and react to the emergence of a particular hazard that must be rapidly addressed. In fact, proper formulation of the auction process, combined with an appropriate update scheme for target priority, potentially retains both the positive features of the combined ant colony / auction approach. While specific sequences are identified for the propsed mission architecture, the two search and coordination algorithms are very general in implementation and are readily applied to many different mission formulations. Specifically, both methods are easily expanded to incorporate alternative propulsion methods such as electric engines and solar sails, long-term relative drift in orbital elements due to harmonic effects, or the modeling and operation of a re-supply depot / “home base” architecture for long-term mitigation potential.

8. Acknowledgements

This research was conducted at Purdue University and the Jet Propulsion Laboratory, California Institute of Technology under contract with the National Aeronautics and Space Administration. The work was supported by a NASA Office of the Chief Technologist’s Space Technology Research Fellowship, NASA Grant NNX12AM61H, and the Purdue Research Foundation. Many thanks to Wayne Schlei, for the many discussion on ACO and auctions, and the technical personnel at the Jet Propulsion Laboratory, Mission Design and Navigation Section. The authors also

acknowledge the contributions of Professor Seokcheon Lee of the Purdue University School of Industrial Engineering.

9. References

[1] Kessler, D. J. and Cour-Palais, B. G. "Collision Frequency of Artificial Satellites: The Creation of a Debris Belt." Journal of Geophysical Research, Vol. 83, No. A6, pp. 2637–2646, 1978.

[2] NASA Orbital Debris Program Office. "Satellite Collision Leaves Significant Debris Clouds." Orbital Debris Quarterly News, Vol. 13, No. 2, pp. 1–2, April 2009.

[3] NASA Orbital Debris Program Office. "Chinese Anit-Satellite Test Creates Most Severe Orbital Debris Cloud in History." Orbital Debris Quarterly News, Vol. 11, No. 2, pp. 2–3, April 2007.

[4] "Satellite Debris Analysis Indicates Hydrazine Tank Hit." U.S. Department of Defense Press Release, February 28 2008. No. 0146-08.

[5] NASA Orbital Debris Program Office. "Fengyun-1C Debris: One Year Later." Orbital Debris Quarterly News, Vol. 12, No. 1, pp. 2–3, January 2008.

[6] Liou, J. "An Active Debris Removal Parametric Study for LEO Environment Remediation." Advances in Space Research, Vol. 47, pp. 1865–1876, 2011.

[7] Loftus, J. P., Anz-Meador, P. D., and Reynolds, R. "Orbital Debris Minimization and Mitigation Techniques." Advances in Space Research, Vol. 13, No. 8, pp. 263–282, 1993.

[8] Lewis, H. G., White, A. E., Crowther, R., and Stokes, H. "Synergy of Debris Mitigation and Removal." Acta Astronautica, Vol. 81, No. 1, pp. 62–68, 2012.

[9] Früh, C., Jah, M., Valdez, E., Kervin, P., and Kelecy, T. "Taxonomy and Classification Scheme for Artificial Space Objects." "Advanced Maui Optical and Space Surveillance Technologies Conference," Maui, Hawaii, September 10-13 2013.

[10] Wilkins, M. P., Pfeffer, A., Schumacher, P. W., and Jah, M. K. "Towards an Artificial Space Object Taxonomy." "Advanced Maui Optical and Space Surveillance Technologies Conference," Maui, Hawaii, September 10-13 2013.

[11] McCall, P. D. "Modeling, Simulation, and Characterization of Space Debris in Low-Earth Orbit." Ph.D. Thesis, Florida International University, Miami, Florida, 2013.

[12] Wiegmann, B. M. "NASA's Marshall Space Flight Center Recent Studies and Technology Developments in the Area of SSA/Orbital Debris." "Advanced Maui Optical and Space Surveillance Technologies Conference," Wailea, Maui, Hawaii, September 11-14 2012.

[13] Peterson, G. E. "Target Identification and Delta-V Sizing for Active Debris Removal and Improved Tracking Campaigns." "23rd International Symposium on Spaceflight Dynamics," Pasadena, California, October 29 - November 2 2012. Paper No. ISSFD23-CRSD2-5.

[14] Castronuovo, M. M. "Active Space Debris Removal - A Preliminary Mission Analysis and Design." Acta Astronautica, Vol. 69, No. 9-10, pp. 848–859, November-December 2011.

[15] Braun, V., Lupken, A., Flegel, S., Gelhaus, J., Mockel, M., Kebschull, C., Wiedemann, C., and Vorsmann, P. "Active debris removal of multiple priority targets." Advances in Space Research, Vol. 51, pp. 1638–1648, 2013.

[16] Missel, J. and Mortari, D. "Path Optimization for Space Sweeper with Sling-Sat: A Method of Sctive Space Debris Removal." Advances in Space Research, Vol. 52, pp. 1339–1348, 2013.

[17] Barbee, B. W., Alfano, S., Pinon, E., Gold, K., and Gaylor, D. "Design of Spacecraft Missions to Remove Multiple Orbital Debris Objects." "35th Annual AAS Guidance and Control Conference," Breckenridge, Colorado, February 3-8 2012.

[18] Ceriotti, M. and Vasile, M. "MGA Trajectory Planning with an ACO-inspired Algorithm." Acta Astronautica, Vol. 67, pp. 1202–1217, 2010.

[19] de Weck, O., Scialom, U., and Siddiqi, A. "Optimal Reconfiguration of Satellite Constellations with the Auction Algorithm." Acta Astronautica, Vol. 62, No. 2, pp. 112–130, 2008.

[20] Salazar, A. and Tsiotras, P. "An auction algorithm for allocating fuel in satellite constellations using peer-to-peer refueling." "2006 American Control Conference," Minneapolis, Minnesota, June 14-16 2006.

[21] Hilland, J., Wessen, R., Porter, D., and Austin, R. "A market-based conflict resolution approach for satellite mission planning." IEEE Transactions on Engineering Management, Vol. 48, No. 3, pp. 272–282, 2001.

[22] Dorigo, M., Maniezzo, V., and Colorni, A. "Positive Feedback as a Search Strategy." Tech. rep., Dipartimento di Elettronica, Politecnico di Milano, Italy, 1991. Tech. Rep. 91-016.

[23] Dorigo, M. and Stützle, T. *Ant Colony Optimization*. MIT Press, Cambridge, Massachusetts, 2004.

[24] Vickrey, W. "Counterspeculation, auction, and competitive sealed tenders." Journal of Finance, Vol. 16, pp. 8–37, 1961.

[25] Varian, H. R. "Economic Mechanism Design for Computerized Agents." "Proceedings of the First USENIX Workshop on Electronic Commerce," New York, New York, July 1995.

[26] Lewis, H. G., Newland, R., Swinerd, G., and Saunders, A. "A New Analysis of Debris Mitigation and Removal Using Networks." Acta Astronautica, Vol. 66, No. 1-2, pp. 257–268, 2010.

[27] Stuart, J. R., Howell, K. C., and Wilson, R. S. "Design of End-To-End Trojan Asteroid Rendezvous Tours Incorporating Potential Scientific Value." "AAS/AIAA 24th Space Flight Mechanics Meeting," Santa Fe, New Mexico, January 26-30 2014. Paper No. AAS-14-267.

[28] Bonabeau, E., Dorigo, M., and Theraulaz, G. *Swarm Intelligence: From Natural to Artificial Systems*. Oxford University Press, Oxford, England, United Kingdom, 1999.

[29] Rizzoli, A., Oliverio, F., Montemanni, R., and Gambardella, L. "Ant Colony Optimisation for vehicle routing problems: from theory to applications." Tech. rep., Instituto Dalle Molle di Studi sull'Intelligenza Artificiale (IDSIA), September 7 2004. IDSIA-15-04.